ARTICLE

BIOTECHNOLOGY and BIOENGINEERING

Effects of Topography on the Functional Development of Human Neural Progenitor Cells

Ze-Zhi Wu,[1,2] William S. Kisaalita,[2] Lina Wang,[2] Angela L. Zachman,[2] Yiping Zhao,[3] Kowser Hasneen,[4] Dave Machacek,[4] Steven L. Stice[4]

[1]Key Laboratory of Biorheological Science and Technology under the State Ministry of Education, "111 Project" Laboratory of Biomechanics and Tissue Repair, College of Bioengineering, Chongqing University, Chongqing, PR China

[2]Cellular Bioengineering Laboratory, Faculty of Engineering, The University of Georgia, Athens, Georgia 30602; telephone: 1-706-542-0835; fax: 1-706-542-8806; e-mail: williamk@engr.uga.edu

[3]Department of Physics and Astronomy, The University of Georgia, Athens, Georgia

[4]Department of Animal and Dairy Science, Regenerative BioScience Center, The University of Georgia, Athens, Georgia

Received 7 October 2009; revision received 12 February 2010; accepted 16 February 2010

Published online 2 March 2010 in Wiley InterScience (www.interscience.wiley.com). DOI 10.1002/bit.22715

ABSTRACT: We have fabricated a topographical substrate with a packed polystyrene bead array for the development of cell-based assay systems targeting voltage-gated calcium channels (VGCCs). Human neural progenitor cells (H945RB.3) cultured on both flat and topographical substrates were analyzed in terms of morphological spreading, neuronal commitment, resting membrane potential (V_m) establishment and VGCC function development. We found, by SEM imaging, that arrayed substrates, formed with both sub-micrometer (of 0.51 μm in mean diameter) and micrometer (of 1.98 μm in mean diameter) beads, were capable of promoting the spreading of the progenitor cells as compared with the flat polystyrene surfaces. With the micrometer beads, it was found that arrayed substrates facilitated the neural progenitor cells' maintenance of less negative V_m values upon differentiation with bFGF starvation, which favored predominant neuronal commitment. Almost all the progenitor cells were responsive to 50 mM K^+ depolarization with an increase in $[Ca^{2+}]_i$ either before or upon differentiation, suggesting the expression of functional VGCCs. Compared to the flat polystyrene surfaces, microbead arrayed substrates facilitated the development of higher VGCC responsiveness by the progenitor cells upon differentiation. The enhancement of both VGCC responsiveness and cell spreading by arrays of micrometer beads was most significant on day 14 into differentiation, which was the latest time point of measurement in this study. This study thus rationalized the possibility for future substrate topography engineering to manipulate ion channel function and to meet the challenge of low VGCC responsiveness found in early drug discovery.

Biotechnol. Bioeng. 2010;106: 649–659.

Correspondence to: W.S. Kisaalita

KEYWORDS: human neural stem/progenitor cells; voltage-gated calcium channel; resting membrane potential; confocal microscopy; substrate topography; microfabrication

Introduction

Surface topography is a major concern in the design of culture substrates for application in cell-based microdevices. A large number of studies have addressed the effects of substrate topography on cellular behaviors, and microscale or sub-microscale topographical features have been designed to promote cell attachment and even differentiation (Craighead et al., 2001; Dalby et al., 2002, 2003; Flemming et al., 1999; Haq et al., 2005; Karuri et al., 2004; Li et al., 2003; Martinez et al., 2009). Neuron-based microdevices have been, to a large extent, based upon and promoted by surface topography engineering since topography has been exploited to pattern cell morphology, to direct neuronal extensions and to create a three-dimensional (3-D) microenvironment (Craighead et al., 2001; Haq et al., 2005; Jimbo et al., 1993; Li et al., 2003; Luo and Shoichet, 2004; Merz and Fromherz, 2002; Wu et al., 2006a). An understanding of the relationship between substrate topography and cell function is thus of pivotal importance for the advancement of neuron-based microdevices and related fields.

Although the effects of surface topography on neuronal cell behaviors have been addressed, very few studies have included an analysis of membrane potential and voltage-gated calcium channels (VGCCs) function. One of the most

important features of neuronal cell differentiation is the establishment of resting membrane potential and expression of characteristic profile of ion channels in a regulated and maturation dependent manner, which serves as markers of functional maturation as well as targets for drug screening. VGCCs are of interest as they are related to a number of central nervous and cardiovascular diseases (Denyer et al., 1998). We have been interested in the development of neuronal cell-based assay systems with topographical scaffolds for early drug discovery targeting VGCCs (Wang et al., 2009; Wu et al., 2006a,b). With the SH-SY5Y human neuroblastoma cells, we found that only a small percentage of the cells were responding to 50 mM K^+ stimulation with an increase in intracellular calcium concentration, indicating low expression of VGCC responsiveness in these cells (Wu et al., 2006b). We also found that cells cultured on the topographical scaffolds were spread less, established more negative resting membrane potentials and showed even lower VGCC responsiveness than cells on flat substrates (Wang et al., 2009; Wu et al., 2006a,b). However, screening systems based upon tumorigenic cells like SH-SY5Y cells are sometimes questioned on grounds of cellular abnormality. Thus, development of assays with neural stem/progenitor cells provides a prospective alternative for early drug discovery against VGCCs. It was reported that neural progenitor cells might exhibit no detectable calcium transient responses upon depolarization stimulation and the VGCC responsiveness became significant only after induction of differentiation (D'Ascenzo et al., 2006). Neural stem/progrnitor cells with robust VGCC responsiveness or measures for enhancing this responsiveness are highly anticipated for the development of such assay systems.

In this study, we evaluated a newly isolated human neural progenitor cell line, namely H945RB.3, as a candidate sensing element for the cell-based assay system targeting VGCC. We hypothesized that VGCC responsiveness of the progenitor cells could be enhanced and cell resting membrane potential (V_m) establishment be shifted to a less negative value by a substrate topography design that promotes cell spreading. We fabricated topographical substrates using a packed array of polystyrene beads of either sub-micrometer (of 0.51 μm in nominal mean diameter) or micrometer (of 1.98 μm in nominal mean diameter) scale. With the micrometer bead arrayed substrates, neuron functional development of the cells was then compared with that for cells on flat substrates in terms of resting membrane potential establishment, VGCC responsiveness as well as early neuronal marker expression in an attempt to understand the effects of microbead topography.

Materials and Methods

Preparation of the Cell Culture Substrates

Cell culture substrates were fabricated on 25-mm coverslips (Fisher Scientific, Pittsburgh, PA). Polystyrene coated flat substrates were fabricated as previously reported (Wu et al., 2006b). To prepare the microbead arrayed substrates, polystyrene beads (Bangs Laboratories, Inc., Fishers, IN) of 0.51 μm and 1.98 ± 0.20 μm in diameter were diluted to a concentration of ~1.7% (w/v) with distilled water and 30 μL bead suspension was spread over the polystyrene coated coverslip. The whole set was tilted approximately 10° and dried in ambient condition for 30 min before large areas of packed bead arrays were formed (Micheletto et al., 1995; Wu et al., 2006b). To stabilize the attachment of the beads to the underlying flat polystyrene surfaces, the arrayed substrates were baked at 104°C for 35 min. Both the flat polystyrene substrates and bead arrayed substrates were then etched with oxygen plasma (PLASMOD™ Oxygen Plasma System, TEGAL Corporation, Richmond, CA) for 150 s to increase the surface roughness. The nano-scale surface topography of the polystyrene surface was examined with a commercial atomic force microscope (AUTOPROBE CP Research, TM Microscopes, Sunnyvale, CA) with a ULNC-AUMT-CD cantilever in non-contact mode both before and after oxygen plasma etching.

The cell culture substrates, either flat or microbeaded, were sterilized with 70% ethanol overnight before washing with distilled water. Substrates/cell culture dishes (FALCON, Beckton Dickinson Labware, NJ) were bath coated with 40 μg/mL polyornithine (Sigma, St. Louis, MO) and 5 μg/mL murine basement membrane laminin (Sigma) each for at least 2 h.

Culture of the Neural Progenitor Cells

H945RB.3 human neural progenitor cells were derived from WA09 human ES cells (Shin et al., 2006), and are now available from Millipore as ENStem-A™. Neural progenitor cells were propagated in 35 mm Petri dishes as previously described (Cheng et al., 2008). For cell differentiation experiments, progenitor cells of passage 25–42 were used in the present study. Cells were seeded in 35 mm Petri dishes containing either a flat or microbead arrayed substrate, in proliferation medium. On day 2 after plating, referred to as day 0 into differentiation (0 DID hereafter), cell differentiation was initiated by changing medium to differentiation medium. The differentiation medium had the same composition as proliferation medium except bFGF was withdrawn (Cheng et al., 2008). Under the present culture condition, this neural progenitor cell line predominantly differentiated into neuronal phenotype. Its specific subphenotype (e.g., neurotransmitter type) has not yet been established.

Scanning Electron Microscopy (SEM)

On days 0 and 14 into differentiation, cells on either flat or bead arrayed substrates were fixed and dehydrated to prepare for SEM scanning (Wang et al., 2009; Wu et al., 2006a). The samples were sputter-coated with gold for 90 s to achieve a coating thickness of about 23 nm. SEM images

were captured with an LEO 982 scanning electron microscope. Cell morphology was measured with a Simple PCI image software (Compix, Inc., Cranberry Township, PA) by tracking the cell contours. Cellular projection area and perimeter were measured by enclosing the cell bodies and lamellipodia. Roundness was defined as $4 \times \pi \times \text{area}/(\text{perimeter})^2$.

Immunocytochemical Staining

On days 0, 7, and 14 into differentiation, neural progenitor cells on flat and microbeaded substrates were stained for the expression of nestin, beta III tubulin (Tuj) and glial fibrillary acidic protein (GFAP) with immunofluorescent staining (Shin et al., 2006). Antibodies used in this study includes: mouse anti-human nestin IgG1 (1:200, Neuromics, Northfield, MN), chicken anti-Tuj IgY (1:1,000, Chemicon, Temecula, CA), mouse anti-GFAP (1:500, Sigma), Alexa Fluor® 488 donkey anti-mouse IgG (H + L) conjugate (1:1,000, Molecular Probes, Inc., Eugene, OR) and Texas Red® dye-conjugated AffiniPure Donkey anti-chicken IgY (1:250, Jackson ImmunoResearch, West Grove, PA). Cells were finally contrast stained with 4′,6-diamidino-2-phenylindole (DAPI, VWR, PA) at a 1:10,000 dilution in distilled water. Fluorescent images were viewed with a Nikon ECLIPSE TE2000-S inverted microscope.

Evaluation of the Resting Membrane Potential (V_m) Establishment and VGCC Responsiveness

Resting membrane potentials of neural progenitor cells on both flat and microbeaded substrates were evaluated with the potentiometric fluorescent dye Tetramethylrhodamine methyl ester (TMRM, Molecular Probes, Inc.) and confocal microscopy. Briefly, cells were loaded with 500 nM TMRM in uncolored Neurobasal medium (Invitrogen, Carlsbad, CA) containing 2% B-27 supplements for 40 min and then scanned with 543 nm Green HeNe laser using a confocal laser-scanning microscope system (PCM-2000, Nikon, Melville, NY). V_m values were determined from the intra/extracellular fluorescence intensity ratios based on the Nernstian distribution of the dye across plasma membrane (Ehrenberg et al., 1988; Loew, 1998; Mao and Kisaalita, 2004). Because the neural progenitor cells were extremely sensitive to treatment with valinomycin, a procedure for correcting the small amount nonpotentiometric binding was not followed in the present study. The following equation was adopted for calculating the V_m values,

$$V_m = -58 \log_{10}\left(\frac{F_{in} - B}{F_{out} - B}\right)(\text{mV}), \quad (1)$$

where F_{in} and F_{out} are the intra- and extracellular fluorescence intensities while B is the background fluorescence intensity, with neutral density filter set at 10%. Measurements were done within defined regions of interests (ROIs). Fluorescence intensities were expressed as average gray level readings, which range from 0 to 255 artificial gray level units with 0 and 255 indicating the highest darkness and brightness, respectively.

On days 0, 7, and 14 into differentiation, VGCC functionality of cells on either flat or microbeaded substrates were evaluated in terms of the calcium influx dynamics in response to high K^+ (50 mM) depolarization (Wang et al., 2009; Wu et al., 2006b). The membrane permeable fluorescent dye, Calcium Green-1, Acetoxymethyl Ester (AM) (Molecular Probes, Inc.), was used to visualize the calcium influx dynamics. Confocal images were continuously captured at a rate of 1 frame per 3 s. While images being captured, cells were depolarized by adding 100 μL of uncolored Neurobasal medium containing high K^+ (500 mM) to achieve a final K^+ concentration of 50 mM. Functional VGCCs were demonstrated by cytosolic calcium concentration increase upon depolarization. This intracellular calcium dynamics was reflected by changes in relative intracellular Calcium Green-1 fluorescence intensities, which were plotted as gray level units against time.

Data Analysis and Statistics

Morphological parameters, V_m values and fractional VGCC response magnitudes were expressed as Mean ± SD. Student's t-test was used for comparisons of the mean values of morphological measurements, membrane potentials and VGCC response magnitudes either between cells on flat and microbeaded substrates or between cells on different differentiation dates. Resting membrane potentials were also presented as frequency distribution histograms and the nonparametric two-sample Kolmogorov–Smirnov test was used for comparison of the V_m frequency distributions. A level of $P < 0.05$ was accepted as statistically significant.

Results

Effects of Microbeaded Topography on the Spreading of Neural Progenitor Cells

Figure 1a and b shows the AFM images of the flat polystyrene substrates before and after oxygen plasma etching, respectively. At nanoscale, oxygen plasma etching resulted in a significant increase in surface roughness, with the root mean square roughness increased from 0.2014 to 0.3291 nm after oxygen plasma etching. The root mean square roughness was defined as the square root of the mean value of the squares of the distance of the points from the image mean value. Figure 1b and d presents the SEM images for the arrays of the 0.51 μm microbeads. The etched surfaces (Fig. 1c and d) significantly favored cell attachment during culture experiments as compared to unetched surfaces, and were thus used in the following studies.

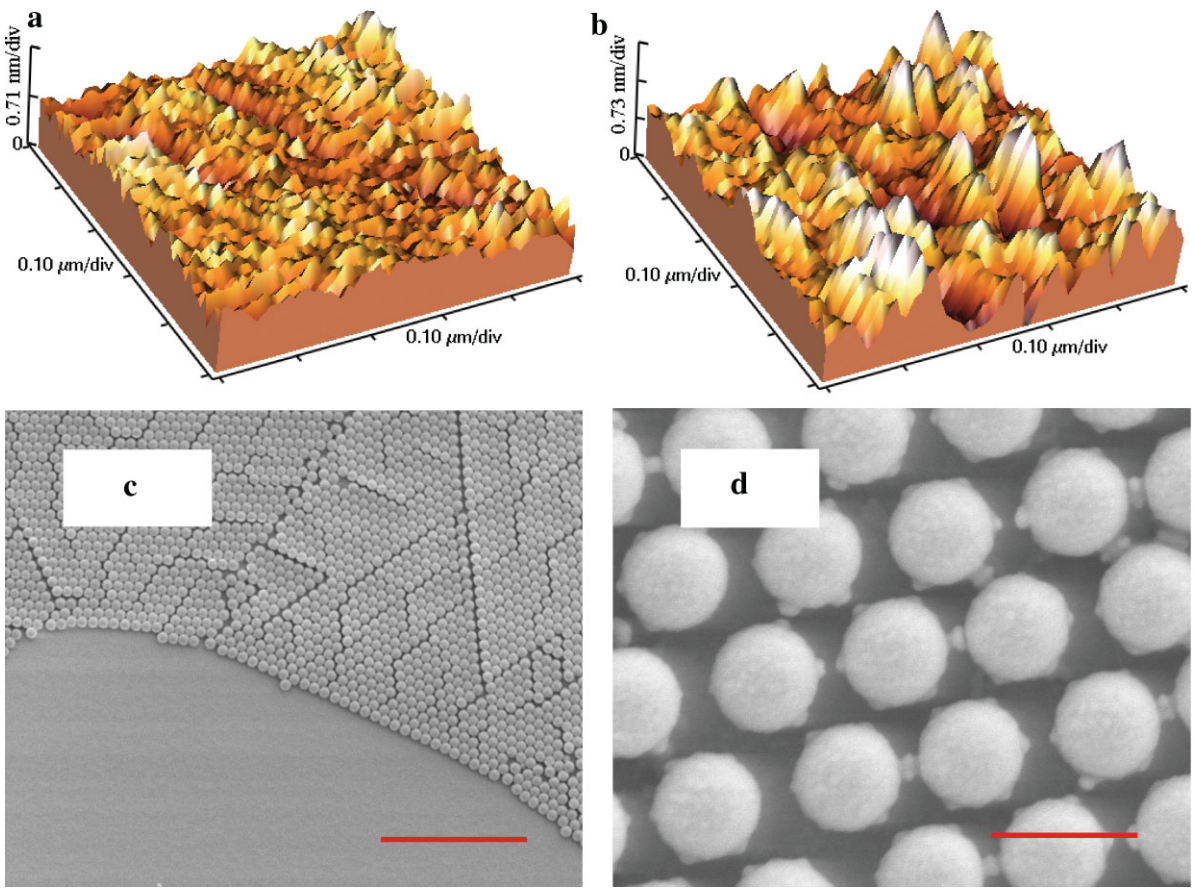

Figure 1. Surface morphology of the flat and bead arrayed substrates. **a** and **b**: AFM images showing the nanoscale topographical features of flat polystyrene surfaces before and after oxygen plasma etching, respectively. **c** and **d**: SEM image showing the array of polystyrene beads with a nominal mean diameter of 0.51 μm. Bar = 6 μm (c) and 0.5 μm (d). [Color figure can be seen in the online version of this article, available at www.interscience.wiley.com.]

After plating, cells grew in similar densities on flat and microbeaded substrates. Cell differentiation was initiated at a confluence of around 60%. Phase contrast images (not presented) showed that, upon differentiation, the progenitor cells gradually stopped proliferation during the first week. Figure 2 presents SEM images for cells on flat (Fig. 2a and d) and microbead arrayed substrates (Fig. 2b, c, e, and f) on days 0 (Fig. 2a–c) and 14 (Fig. 2d, e, and f) into differentiation. It was found from the images that, on day 0 into differentiation, cells were well attached and spread on both flat and bead arrayed substrates (Fig. 2a–c). On day 14 into differentiation, cells were weakly attached and less spread on the flat substrates with extensive peeling off upon preparation for SEM (Fig. 2d). In contrast, cells on beaded substrates, with either the 1.98 or 0.51 μm beads, remained well attached and spread (Fig. 2e and f).

For a further understanding of the effects of microbeaded topography on neural progenitor cell spreading, a cell morphological measurement over the SEM images is shown in Table I. There was a significant decrease in cell projection area and roundness from days 0 to 14 into differentiation for cells on both flat and topographical substrates ($P < 0.01$). On day 0 into differentiation, cells on flat substrates and the 1.98 μm bead arrays had similar projection areas ($P > 0.05$) while cells on the 0.51 μm bead arrays had larger projection areas than cells on both flat substrates and the 1.98 μm bead arrays ($P < 0.01$). On day 14 into differentiation, cells on the 1.98 μm bead arrays had greater projection area ($P < 0.05$) than cells on flat substrates, and cells on the 0.51 μm bead arrays had even larger projection areas than cells on both flat substrates and the 1.98 μm bead arrays ($P < 0.01$). To clearly show the enhancement of cell spreading by microbeaded topography, cell projection areas were normalized to those for cells on flat substrates on day 0 into differentiation and the normalized means were summarized in Figure 3. From Table I and Figures 2 and 3, cell spreading enhancement was only significant on day 14 for the 1.98 μm bead arrays. While for the 0.51 μm bead arrays, such enhancement was significant either before differentiation or on day 14 into differentiation.

Immunocytochemical Staining for the Progenitor, Neuronal, and Astrocyte Markers

Figure 4 presents the immunofluorescent images of the neural progenitor cells on flat substrates (a, c, and e) and the

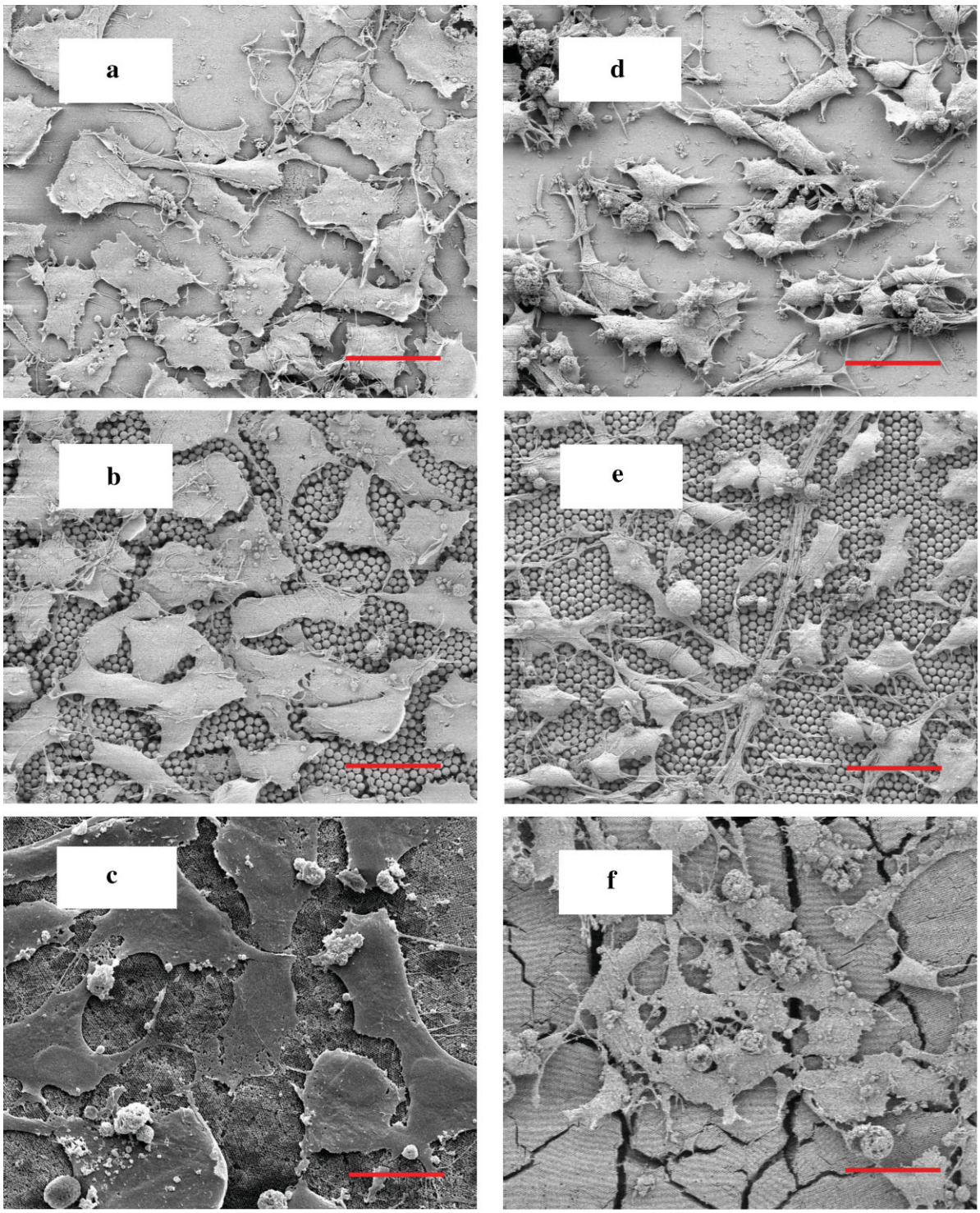

Figure 2. SEM images of H945RB.3 cells growing on flat polystyrene surfaces (**a** and **d**) and microbead arrays (**b**, **c**, **e**, and **f**). The microbeads in had a nominal mean diameter of 1.98 μm in (b) and (e), and 0.51 μm in (c) and (f). Images in the left column (a–c) show cells before differentiation, images in the right column show cells on day 14 into differentiation (d–f). The cracking in (f) happened in the SEM preparation during critical point drying; and this happened more frequently with the 0.51 μm beads than with the 1.98 μm beads. Bar = 20 μm. [Color figure can be seen in the online version of this article, available at www.interscience.wiley.com.]

Table I. Summary of morphological measurements for H945RB.3 neural progenitor cells on flat surfaces and microbead arrays.

	0 DID			14 DID		
	Area (μm^2)	Perimeter (μm)	Roundness	Area (μm^2)	Perimeter (μm)	Roundness
Flat surfaces	262 ± 108 ($n = 249$)	84 ± 25 ($n = 249$)	0.48 ± 0.13 ($n = 249$)	$120 \pm 48^{**}$ ($n = 134$)	87 ± 31 ($n = 134$)	$0.23 \pm 0.10^{**}$ ($n = 134$)
Arrays of 1.98 μm beads	264 ± 131 ($n = 263$)	$90 \pm 34^{\#\#}$ ($n = 263$)	$0.44 \pm 0.14^{\#\#}$ ($n = 263$)	$135 \pm 73^{**,\#}$ ($n = 210$)	$98 \pm 50^{**,\#\#}$ ($n = 210$)	$0.22 \pm 0.10^{**}$ ($n = 210$)
Arrays of 0.51 μm beads	$359 \pm 96^{\#\#,++}$ ($n = 169$)	$105 \pm 19^{\#\#,++}$ ($n = 169$)	$0.42 \pm 0.10^{\#\#,+}$ ($n = 169$)	$168 \pm 50^{**,\#\#,++}$ ($n = 169$)	$81 \pm 22^{**,\#,++}$ ($n = 169$)	$0.35 \pm 0.11^{**,\#\#,++}$ ($n = 169$)

DID, days into differentiation. Differentiation was initiated on day 2 after plating (0 DID). Roundness is defined as $4 \times \pi \times$ area/(perimeter)^2. Measurement was based on SEM images. The perimeter was drawn to enclose the cell body and lamellipodia. Compared with those for day 0 into differentiation: $^{*}P < 0.05$; $^{**}P < 0.01$. Compared with those for cells on flat substrates: $^{\#}P < 0.05$; $^{\#\#}P < 0.01$. Compared with those for cells on the 1.98 μm bead arrays: $^{+}P < 0.05$; $^{++}P < 0.01$. n, number of cells measured.

1.98 μm bead arrays (b, d, and f) stained for markers of the neural progenitor cells (nestin, green) and postmitotic neurons (Tuj, red) on days 0 (a and b), 7 (c and d) and 14 (e and f) into differentiation. It was found that cells on both flat and microbeaded substrates were stained positive for nestin while negative for Tuj before differentiation. On day 7 into differentiation, a large number of cells were stained positive for Tuj and the Tuj staining mostly co-localized with that of nestin. On day 14 into differentiation, Tuj positive neuronal extensions became more significant and the Tuj staining was mostly found to have separated from the nestin staining. No positive staining for the astrocyte marker GFAP was found for the progenitor cells on either day 0, 7, or 14 into differentiation (data not shown). In general, similar staining patterns for nestin, Tuj, and GFAP were noted between neural progenitor cells on flat polystyrene surfaces and those on microbead arrays.

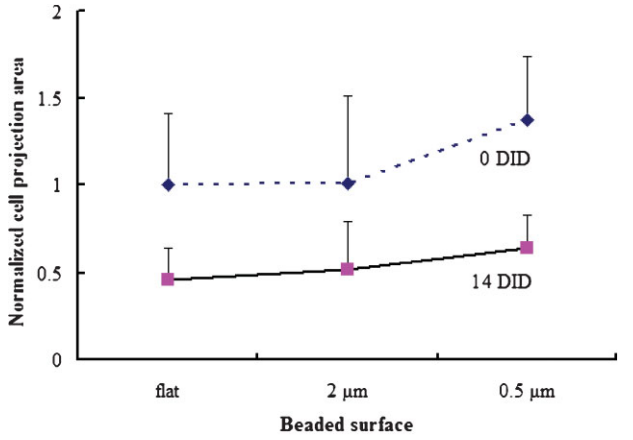

Figure 3. Plot of normalized means of projection areas for cells on flat surfaces, the 1.98 μm and the 0.51 μm bead arrays on days 0 and 14 into differentiation, based on morphological measurements shown in Table I. The means and standard errors were normalized by the mean of projection areas for cells on flat surfaces on day 0 into differentiation. [Color figure can be seen in the online version of this article, available at www.interscience.wiley.com.]

Resting Membrane Potential Establishment

Table II summarizes the resting membrane potential (V_m) values for neural progenitor cells in a period of 14 days into differentiation. It was found that on day 0 into differentiation, cells on the 1.98 μm microbead arrays had significantly more negative V_m values than cells on flat substrates ($P < 0.01$). Upon differentiation, the V_m values for cells on flat surfaces became more negative, while the polarization of V_m values is insignificant for cells on microbead arrays. For either days 7 or 14 into differentiation, cells on microbead arrayed substrates had less negative V_m values than cells on flat substrates ($P < 0.01$).

To further understand the changes in the resting membrane potential establishment, V_m values were presented as frequency distribution (Fig. 5) and the nonparametric two-sample Kolmogorov–Smirnov test was used for comparison of the V_m value frequency distributions for cells cultured on flat and microbeaded substrates. Before differentiation, 49.5% of cells on flat substrates had developed V_m values more negative than -70 mV, a value that was comparable to that described for mature neurons (Owens et al., 1996). Upon differentiation, this percentage increased to 97.7% on day 7 ($P < 0.01$) and 96.5% on day 14 into differentiation ($P < 0.01$). For microbeaded substrates, 80.2% of the cells were more negative than -70 mV before differentiation and this percentage was significantly higher than the corresponding value for cells on flat substrates ($P < 0.01$). Upon differentiation, this percentage increased to 88.4% on day 7 ($P < 0.01$) and 89.6% on day 14 into differentiation ($P < 0.05$). The nonparametric statistical analysis also confirmed the t-test conclusion that microbead arrayed substrates helped cells maintain less negative V_m values as compared with cells on flat substrates, both on days 7 and 14 into differentiation ($P < 0.01$).

VGCC Responsiveness for the Neural Progenitor Cells

Figure 6a and b shows laser scanning confocal microscopic images of neural progenitor cells before (a) and after (b) depolarization. Figure 6c presents a typical time course for the change in cellular Calcium Green-1 fluorescent intensity

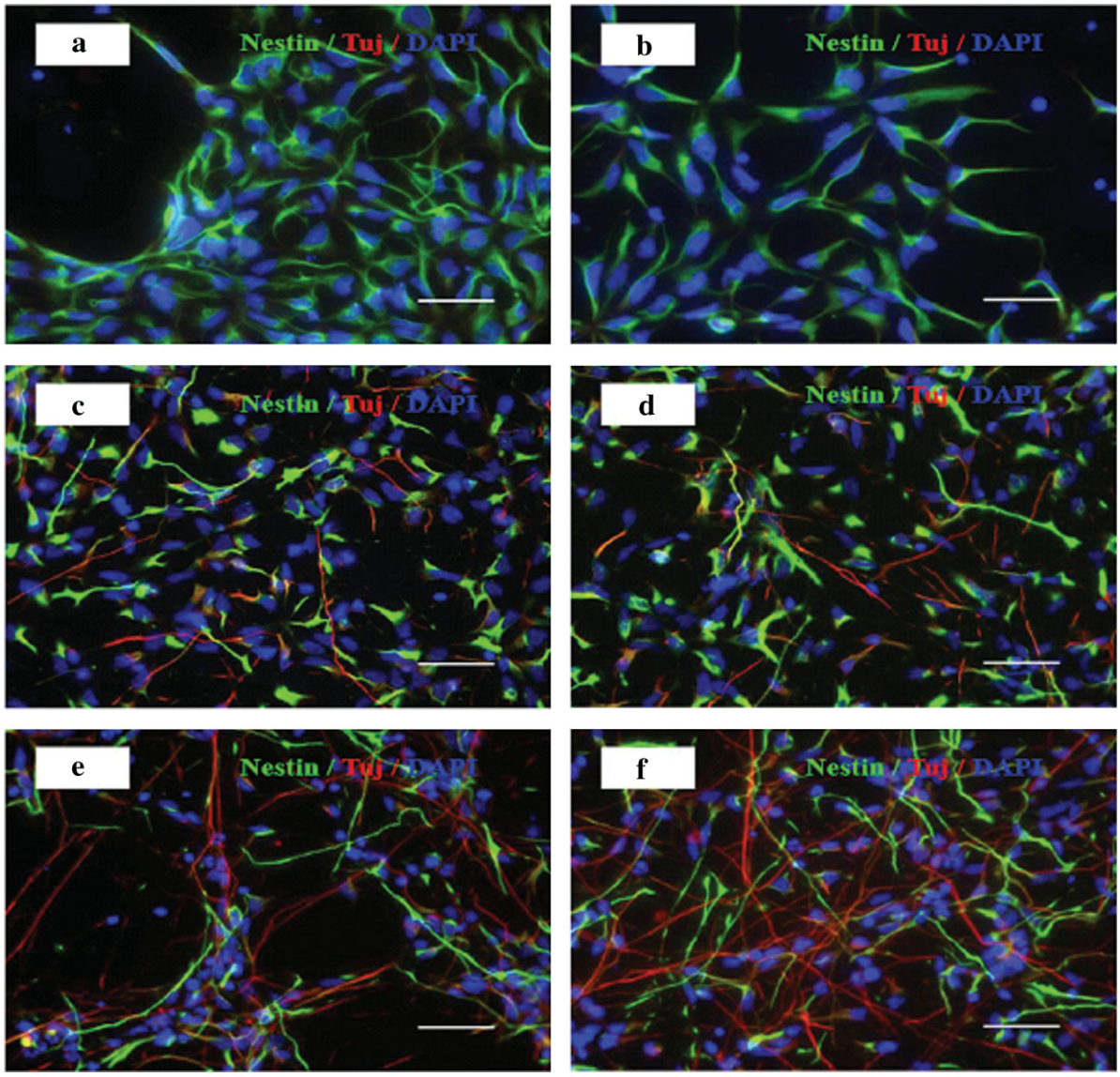

Figure 4. Immunofluorescent staining of the H945RB.3 progenitor cells on flat surfaces (**a**, **c**, and **e**) and the 1.98 μm microbead arrays (**b**, **d**, and **f**) for nestin (green) and Tuj (red) on days 0 (a and b), 7 (c and d) and 14 (e and f) into differentiation. Cells are counter stained with DAPI to show the neuclei (blue). Bar = 40 μm.

upon depolarization. A cell was only considered responsive when it showed an increase in Calcium Green-1 fluorescent intensity of 15% or higher over the basal fluorescent intensity level. We found that near 100% of the neural progenitor cells on both flat and topographical substrates were responsive, either before or after differentiation, indicating the expression of functional VGCCs. The response magnitude or the peak fractional increase over the basal Calcium Green-1 fluorescent intensity was used as an index of VGCC functionality. Table III summarizes the

Table II. Resting membrane potentials of H945RB.3 neural progenitor cells on flat polystyrene substrates and microbead arrayed substrates.

	0 DID	7 DID	14 DID
Flat surfaces (mV)	-71.7 ± 28.9 ($n = 194$)	$-98.1 \pm 14.0^{*}$ ($n = 431$)	$-92.8 \pm 13.6^{*}$ ($n = 372$)
Bead arrays (mV)	$-85.7 \pm 16.3^{\#}$ ($n = 197$)	$-86.5 \pm 13.0^{\#}$ ($n = 439$)	$-83.9 \pm 11.7^{\#}$ ($n = 241$)

DID, days into differentiation. Differentiation was initiated on day 2 after plating (0 DID). The arrayed substrates were fabricated with beads of 1.98 μm in diameter. Compared with those at day 0 into differentiation: $^{*}P < 0.01$. Compared with those for cells on flat substrates: $^{\#}P < 0.01$. *n*, number of cells measured.

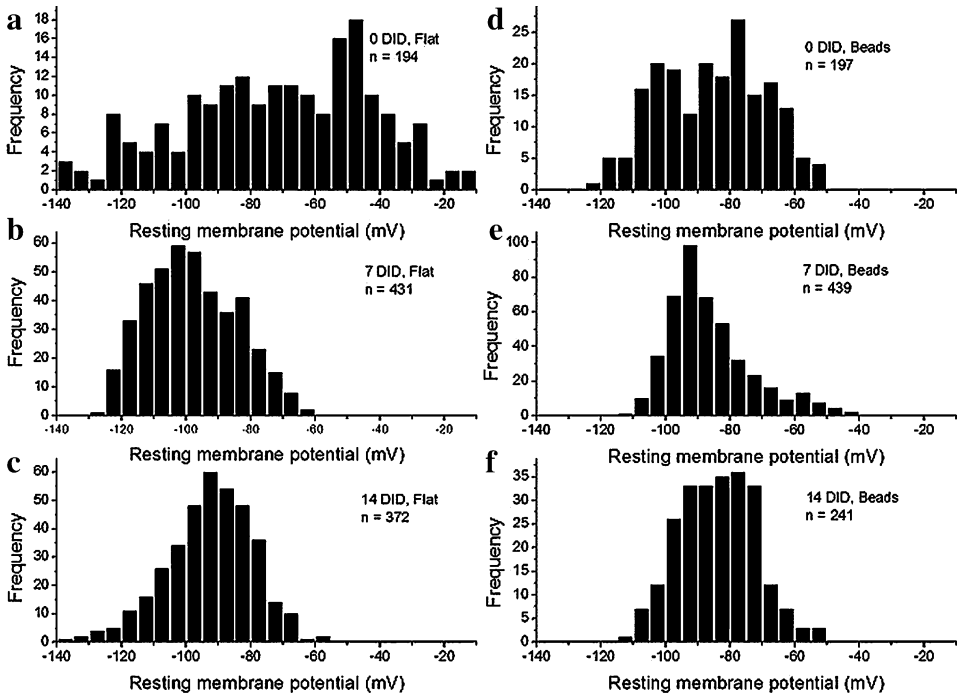

Figure 5. Frequency distribution for the resting membrane potentials of H945RB.3 neural progenitor cells cultured on flat substrates (**a**–**c**) and the 1.98 μm bead arrays (**d**–**f**) on days 0 (a and d), 7 (b and e) and 14 (c and f) into differentiation. Statistical analysis with the nonparametric two-sample Kolmogorov–Smirnov test showed that, before differentiation, cells on microbeaded substrates had more negative V_m values than cells on flat substrates ($P < 0.01$). Upon differentiation, cells on microbeaded substrates maintained less negative V_m values as compared with those for cells on flat substrates, either on days 7 or 14 into differentiation ($P < 0.01$).

response magnitudes. It was found that before differentiation the response magnitudes for cells on microbead arrays (0.88 ± 0.70) were not significantly different from those for cells on flat surfaces (0.86 ± 0.46) ($P > 2.5$). For cells on flat substrates, these values remained at a similar level till day 7 into differentiation (0.90 ± 0.43, $P > 2.5$), but more than doubled by day 14 into differentiation (2.09 ± 1.35, $P < 0.01$). For cells on microbead arrays, the response magnitudes increased significantly on day 7 into differentiation (1.07 ± 0.57, $P < 0.05$) and even further quadrupled on day 14 into differentiation (4.05 ± 2.56, $P < 0.01$). For either days 7 or 14 into differentiation, the response magnitudes were higher for cells on microbead array than those on flat substrates ($P < 0.01$). These results suggest that the microstructured topography formed with the bead arrays promoted the development of VGCC responsiveness, especially on day 14 into differentiation.

Discussion

We fabricated a microbeaded topographical substrate with a simple tilting angle method (Micheletto et al., 1995) to address the effects of surface topography on the functional development of neural progenitor cells. This fabrication method entails no specific instrumentation and enables easy mass production when compared to techniques adapted from the semi-conductor industry. Culture dishes for cell-based assays in drug discovery as well as basic biological research can be prepared with similar procedure (Obeso and Auerbach, 1984; Wu et al., 2006b). Our cell culture experiments with H945RB.3 neural progenitor cells also showed that the present bead arrayed substrates were stable under the fluid mechanical forces of culture handling in a period of more than 2 weeks, with no bead suspension or taken-up by cells. Imperfect bead arrays, such as cracking shown in Figure 2f, occurred in the SEM preparation during critical point drying. Because this cracking of substrates happened after the cells were fixed, it did not compromise the cell morphological measurement. Also, since the cracking happened more frequently with the 0.51 μm- than with the 1.98 μm-beads, the following studies were carried out with the 1.98 μm beads.

Cell morphology is a critical cell biological behavior that responds to substrate topography (Ingber, 1997). Spreading is a direct result of cell–substrate attachment and can thus activate downstream signaling events and lead to other effects of cell–substrate interaction, such as ion channel function, differentiation and even gene expression (Ingber, 1997; Park et al., 2007; Walsh and Parks, 2002). Studies have reported that nanometer or submicrometer scale topographical substrates supported cell attachment and spreading (Dalby et al., 2002, 2003). Our results are consistent with these studies, and showed that the present microbead

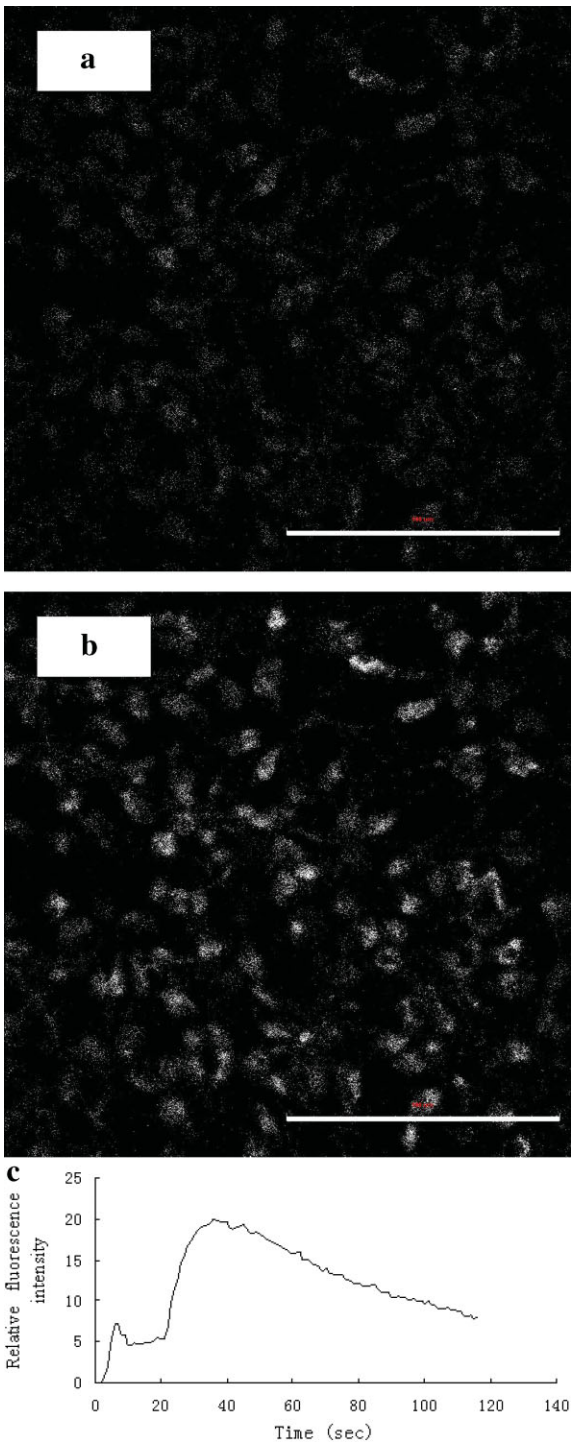

Figure 6. **a** and **b**: Confocal images of H945RB.3 neural progenitor cells before (a) and after (b) 50 mM K^+ stimulation. Cells were cultured on the 1.98 μm bead arrays till day 14 into differentiation (14 DID) and loaded with 5 μM Calcium Green-1 AM in uncolored Neurobasal. **c**: Typical time course for the change in cellular Calcium Green-1 fluorescent intensity upon 50-mM K^+ depolarization. The high K^+ solution was added at around 55 s. The fluctuation at the beginning of the curve represents artifacts due to focusing. © 2009 IEEE. Adapted, with permission, from: Wu Z-Z, Kisaalita WS, Wang L, Zhao Y-P. Microstructured topography enhanced the responsiveness of voltage-gated calcium channels in H945RB.3 human neural progenitor cells. 3rd International Conference on Bioinformatics and Biomedical Engineering (iCBBE 2009). Beijing, China. June 11–16, 2009.

topographical substrates promoted the morphological spreading of neural progenitor cells, fulfilling our original design expectation. In addition, a general relation between substrate topography and cell morphology has been established in this study. The disagreement between changes in perimeter versus projection area for cells on the 1.98 μm beads and 0.51 μm beads at 14 DID suggested that cells on the larger beads had stronger neurite formation and were thus less "round" than cells on smaller beads, which is consistent with the roundness parameter. One possible explanation of the cell spreading enhancement on microbead arrays may be due to the accelerated integrin clustering/focal contact formation compared to smooth surface (Park et al., 2007).

The analysis of resting membrane potential establishment showed that all neural progenitor cells developed detectable negative resting membrane potentials. This is in contrast to neuroblastoma cells where a number of cells had "positive" V_m values (Desai et al., 2006; Mao and Kisaalita, 2004; Wu et al., 2006a,b). This is probably due to the fact that the neural progenitor cells were extremely sensitive to treatment with valinomycin, and therefore a correction for nonspecific dye binding applied to neuroblastoma cells was not possible. However, V_m values obtained were in agreement with those reported for neural progenitor cells or precursor derived neural cells with the patch clamp technique (Hogg et al., 2004; Pagani et al., 2006). We thus expect that this does not compromise the comparative conclusions reached. Studies have showed that the negative V_m values first increased and then decreased or leveled off during differentiation (Herberth et al., 2002; Liu et al., 1999; Moe et al., 2005; Westerlund et al., 2003; Wislet-Gendebien et al., 2005). From the temporal profile of the ionic channel expression, the increase in the negative V_m values most probably reflected the development of the resting K^+ channel currents while the shift of V_m to a less negative value most probably reflected the development of the voltage-gated Na^+ channels and resting Na^+ permeability (Cho et al., 2002; Hogg et al., 2004; Piper et al., 2000). The development of voltage-gated Na^+ channels has been considered as a characteristic of functional maturation which is related to the development of resting membrane potentials, action potential firing and VGCC responsiveness (Balasubramaniyan et al., 2004; Cho et al., 2002; Hogg et al., 2004; Pagani et al., 2006; Piper et al., 2000). Although a quantitative relation between the V_m and the projection area has not been established, it is reasonable to speculate that enhancement of morphological spreading by microbead arrayed substrates is related to the shift of V_m to less negative values. Enhancement of cell spreading can result in change in membrane capacitance and trigger stretching-activated conductance, both of which can contribute to shift of the resting membrane potentials (Iwasa, 1993; Nishimura et al., 2008).

Previous studies with SH-SY5Y human neuroblastoma cells showed that only small percentage of the cells developed VGCC responsiveness with 50 mM K^+ depolarization (Desai et al., 2006; Wang et al., 2009; Wu et al.,

Table III. Response magnitudes for the increase of Calcium Green-1 fluorescent intensities of H945RB.3 neural progenitor cells upon stimulation with 50 mM potassium.

	0 DID	7 DID	14 DID
Cells on flat surface	0.86 ± 0.46 ($n = 54$)	0.90 ± 0.43 ($n = 60$)	$2.09 \pm 1.35^{**}$ ($n = 51$)
Cells on bead array	0.88 ± 0.70 ($n = 73$)	$1.07 \pm 0.57^{\#,*}$ ($n = 280$)	$4.05 \pm 2.56^{\#,**}$ ($n = 102$)

DID, days into differentiation. Differentiation was initiated on day 2 after plating (0 DID). The arrayed substrates were fabricated with beads of 1.98 μm in diameter. Compared with those at day 0 into differentiation (before differentiation): $^{*}P < 0.05$; $^{**}P < 0.01$. Compared with those for cells on flat surfaces: $^{\#}P < 0.01$. *n*, number of cells measured.

2006b). In mice cortical neural progenitor cells, it was reported that there was no detectable calcium transient responses upon depolarization stimulation and the VGCC responsiveness became significant only after 12 days of differentiation induction (D'Ascenzo et al., 2006). Our results with H945RB.3 neural progenitor cells were in contrast with those found with SH-SY5Y cells and mice cortical neural progenitor cells in that robust VGCC responsiveness was observed even before induction of differentiation. In this regard, the use of H945RB.3 neural progenitor cells may provide a prospective alternative for the development of cell-based assay systems targeting VGCC for early drug discovery, due to their expansion and differentiation capabilities as well as higher VGCC responsiveness.

Our experimental finding that the microstructured substrate topography formed with a packed microbead array helped maintain a less negative V_m value and enhanced the development of VGCC responsiveness for the progenitor cells demonstrated the feasibility of using surface topography engineering for manipulating VGCC responsiveness. The enhancement of cell spreading (Table I and Figs. 2 and 3) and VGCC responsiveness (Table III) by the 1.98 μm bead arrays suggests that the VGCC responsiveness might be related to cell morphological spreading, especially on day 14 into differentiation. In a recent study, the same neural progenitor cells were used and it was found that cells cultured on a 3-D porous scaffold were spread less and had lower VGCC responsiveness, as judged by calcium response magnitudes, than cells on 2-D flat substrates (Cheng et al., 2008). This is consistent with the present results on the possible relation between VGCC responsiveness and morphological spreading of the neural progenitor cells. Furthermore, this is in keeping with studies with cardiac myocytes where changes in cell morphology strongly affected the properties of voltage-gated ion channels (Walsh and Parks, 2002). This study thus rationalized the feasibility of substrate topography engineering for manipulating neuron functional establishment and added to the novelty of using neural progenitor cells for the development of cell-based assay systems targeting VGCCs.

Conclusions

Microstructured topographical substrates formed with a packed polystyrene bead array were a stable and appropriate scaffold for the development of cell-based assay systems. These substrates, formed with either submicrometer (of 0.51 μm in diameter) or micrometer (of 1.98 μm in diameter) beads, were capable of promoting the morphological spreading of H945RB.3 human neural progenitor cells as compared with the flat polystyrene surfaces. It was found that almost all the progenitor cells were responsive to 50 mM K^+ depolarization with a robust increase in intracellular calcium concentration either before or after differentiation, suggesting the expression of functional VGCCs. Compared to the flat polystyrene surfaces, microbead arrayed substrates yielded neural progenitor cells with less negative V_m values and higher VGCC responsiveness while had no significant effect on the staining pattern of nestin, Tuj and GFAP, suggesting that these cells were functionally different from those on flat substrates.

These results showed that H945RB.3 human neural progenitor cells were appropriate candidate cells for the development of cell-based assay systems targeting VGCCs for early drug discovery. Also, the present study rationalized the feasibility of substrate topography engineering for manipulating neuron functional establishment and adding to the novelty of using neural progenitor cells for the development of such systems.

The authors are indebt to Dr. Nolan Boyd in the Department of Animal and Dairy Science, Regenerative BioScience Center, The University of Georgia, for technical support. Part of the results have appeared in: Z.-Z. Wu, W.S. Kisaalita, L. Wang, Y.-P. Zhao, Microstructured topography enhanced the responsiveness of voltage-gated calcium channels in H945RB.3 human neural progenitor cells. 3rd International Conference on Bioinformatics and Biomedical Engineering (iCBBE 2009). Beijing, China. June 11-16, 2009. © 2009 IEEE. Reuse of the data was kindly granted.

References

Balasubramaniyan V, de Haas AH, Bakels R, Koper A, Boddeke HWGM, Copray JM. 2004. Functionally deficient neuronal differentiation of mouse embryonic neural stem cells in vitro. Neurosci Res 49(2):261–265.

Cheng K, Lai YZ, Kisaalita WS. 2008. Three-dimensional polymer scaffolds for high throughput cell-based assay systems. Biomaterials 29(18): 2802–2812.

Cho T, Bae JH, Choi HB, Kim SS, McLarnon JG, Suh-Kim H, Kim SU, Min CK. 2002. Human neural stem cells: Electrophysiological properties of voltage-gated ion channels. Neuroreport 13(11):1447–1452.

Craighead HG, James CD, Turner AMP. 2001. Chemical and topographical patterning for directed cell attachment. Curr Opin Solid State Mater Sci 5(2–3):177–184.

Dalby MJ, Riehle MO, Johnstone HJ, Affrossman S, Curtis AS. 2002. Polymer-demixed nanotopography: Control of fibroblast spreading and proliferation. Tissue Eng 8(6):1099–1108.

Dalby MJ, Riehle MO, Johnstone HJH, Affrossman S, Curtis ASG. 2003. Nonadhesive nanotopography: Fibroblast response to poly(n-butyl methacrylate)-poly(styrene) demixed surface features. J Biomed Mater Res A 67(3):1025–1032.

D'Ascenzo M, Piacentini R, Casalbore P, Budoni M, Pallini R, Azzena GB, Grassi C. 2006. Role of L-type Ca2+ channels in neural stem/progenitor cell differentiation. Eur J Neurosci 23(4):935–944.

Denyer J, Worley J, Cox B, Allenby G, Banks M. 1998. HTS approaches to voltage-gated ion channel drug discovery. Drug Discov Today 3(7): 323–332.

Desai A, Kisaalita WS, Keith C, Wu ZZ. 2006. Human neuroblastoma (SH-SY5Y) cell culture and differentiation in 3-D collagen hydrogels for cell-based biosensing. Biosens Bioelectron 21(8):1483–1492.

Ehrenberg B, Montana V, Wei MD, Wuskell JP, Loew LM. 1988. Membrane potential can be determined in individual cells from the nernstian distribution of cationic dyes Biophys J 53(5):785–794.

Flemming RG, Murphy CJ, Abrams GA, Goodman SL, Nealey PF. 1999. Effects of synthetic micro- and nano-structured surfaces on cell behavior. Biomaterials 20(6):573–588.

Haq F, Rao YL, Keith C, Zhao YP, Zhang GG. 2005. Nano- and micro-structured substrates for neuronal cell development. J Biomed Nanotechnol 1(3):313–319.

Herberth B, Pataki A, Jelitai M, Schlett K, Deak F, Spat A, Madarasz E. 2002. Changes of KCl sensitivity of proliferating neural progenitors during in vitro neurogenesis. J Neurosci Res 67(5):574–582.

Hogg RC, Chipperfield H, Whyte KA, Stafford MR, Hansen MA, Cool SM, Nurcombe V, Adams DJ. 2004. Functional maturation of isolated neural progenitor cells from the adult rat hippocampus. Eur J Neurosci 19(9):2410–2420.

Ingber DE. 1997. Engineering cell shape and function through control of substrate adhesion. In: Mittal KL, Lee K-W, editors. Polymer surfaces and interfaces: Characterization, modification and application. Utrecht, The Netherlands: VSP, p 413–424.

Iwasa KH. 1993. Effect of stress on the membrane capacitance of the auditory outer hair cell. Biophys J 65(1):492–498.

Jimbo Y, Robinson HP, Kawana A. 1993. Simultaneous measurement of intracellular calcium and electrical activity from patterned neural networks in culture. IEEE Trans Biomed Eng 40(8):804–810.

Karuri NW, Liliensiek S, Teixeira AI, Abrams G, Campbell S, Nealey PF, Murphy CJ. 2004. Biological length scale topography enhances cell-substratum adhesion of human corneal epithelial cells. J Cell Sci 117(Pt 15):3153–3164.

Li N, Tourovskaia A, Folch A. 2003. Biology on a chip: Microfabrication for studying the behavior of cultured cells. Crit Rev Biomed Eng 31(5–6): 423–488.

Liu RH, Morassutti DJ, Whittemore SR, Sosnowski JS, Magnuson DS. 1999. Electrophysiological properties of mitogen-expanded adult rat spinal cord and subventricular zone neural precursor cells. Exp Neurol 158(1):143–154.

Loew LM. 1998. Measuring membrane potential in single cells with confocal microscopy. In: Celis JE, editor. Cell biology, a laboratory handbook, 2nd edn. San Diego, London, New York, Sidney, Tokyo, Toronto: Academic Press, p 375–379.

Luo Y, Shoichet MS. 2004. A photolabile hydrogel for guided three-dimensional cell growth and migration. Nature Mater 3(4):249–253.

Mao C, Kisaalita WS. 2004. Determination of resting membrane potential of individual neuroblastoma cells (IMR-32) using a potentiometric dye (TMRM) and Confocal Microscopy. J Fluorescence 14(6):739–743.

Martinez E, Engel E, Planell JA, Samitier J. 2009. Effects of artificial micro- and nano-structured surfaces on cell behaviour. Ann Anat 191(1):126–135.

Merz M, Fromherz P. 2002. Polyester microstructures for topographical control of outgrowth and synapse formation of snail neurons. Adv Mater 14(2):141–144.

Micheletto R, Fukuda H, Ohtsu M. 1995. A simple method for the production of a two-dimensional, ordered array of small latex particles. Langmuir 11(9):3333–3336.

Moe MC, Varghese M, Danilov AI, Westerlund U, Ramm-Pettersen J, Brundin L, Svensson M, Berg-Johnsen J, Langmoen IA. 2005. Multipotent progenitor cells from the adult human brain: Neurophysiological differentiation to mature neurons. Brain 128(Pt 9):2189–2199.

Nishimura S, Seo K, Nagasaki M, Hosoya Y, Yamashita H, Fujita H, Nagai R, Sugiura S. 2008. Responses of single-ventricular myocytes to dynamic axial stretching. Prog Biophys Mol Biol 97(2–3):282–297.

Obeso JL, Auerbach R. 1984. A new microtechnique for quantitating cell movement in vitro using polystyrene bead monolayers. J Immunol Methods 70(2):141–152.

Owens DF, Boyce LH, Davis MB, Kriegstein AR. 1996. Excitatory GABA responses in embryonic and neonatal cortical slices demonstrated by gramicidin perforated-patch recordings and calcium imaging. J Neurosci 16(20):6414–6423.

Pagani F, Lauro C, Fucile S, Catalano M, Limatola C, Eusebi F, Grassi F. 2006. Functional properties of neurons derived from fetal mouse neurospheres are compatible with those of neuronal precursors in vivo. J Neurosci Res 83(8):1494–1501.

Park J, Bauer S, von der Mark K, Schmuki P. 2007. Nanosize and vitality: TiO2 nanotube diameter directs cell fate. Nano Lett 7(6):1686–1691.

Piper DR, Mujtaba T, Rao MS, Lucero MT. 2000. Immunocytochemical and physiological characterization of a population of cultured human neural precursors. J Neurophysiol 84(1):534–548.

Shin SJ, Mitalipova M, Noggle S, Tibbitts D, Venable A, Rao R, Stice SL. 2006. Long-term proliferation of human embryonic stem cell-derived neuroepithelial cells using defined adherent culture conditions. Stem Cells 24(1):125–138.

Walsh KB, Parks GE. 2002. Changes in cardiac myocyte morphology alter the properties of voltage-gated ion channels. Cardiovasc Res 55(1): 64–75.

Wang L, Wu ZZ, Xu BQ, Zhao YP, Kisaalita WS. 2009. SU-8 microstructure for quasi-three-dimensional cell-based biosensing. Sensor Actuat B Chem 140(2):349–355.

Westerlund U, Moe MC, Varghese M, Berg-Johnsen J, Ohlsson M, Langmoen IA, Svensson M. 2003. Stem cells from the adult human brain develop into functional neurons in culture. Exp Cell Res 289(2):378–383.

Wislet-Gendebien S, Hans G, Leprince P, Rigo JM, Moonen G, Rogister B. 2005. Plasticity of cultured mesenchymal stem cells: Switch from nestin-positive to excitable neuron-like phenotype. Stem Cells 23(3): 392–402.

Wu ZZ, Zhao YP, Kisaalita WS. 2006a. Interfacing SH-SY5Y human neuroblastoma cells with SU-8 microstructures. Colloid Surf B-Biointerfaces 52(1):14–21.

Wu ZZ, Zhao YP, Kisaalita WS. 2006b. A packed Cytodex microbead array for three-dimensional cell-based biosensing. Biosens Bioelectron 22(5): 685–693.